A Comparative Study on Ionospheric Parameter Measured with Ionosonde and Predicted using IRIPLAS-2011 Model during Earthquake at Mid and Low Latitude

Harleen.Kaur[1], Shival.Verma[1] and Pramod.Kumar.Purohit [2]

[1] Department of Physics, Barkatullah University, Bhopal. (M.P) (India) - 462026.

[2]National Institute of Technical Teacher's Training and Research, Bhopal. (M.P) (India) - 462 002.

ABSTRACT

This paper presents a comparative study on the important parameter of the ionosphere critical frequency of F2 layer (foF2) retrieved by means of ground based ionosonde radars and predicted by International Reference Ionosphere extended till plasma sphere (IRIPLAS-2011) model at two different locations including Northern Sumatra (Geographic Lat. 2.311°N,Geographic Long. 93.063°E) and Fox Island, Alaska (Geographic Lat. 52.008°N, Geographic Long.171.859°W) in the low and mid latitude during the earthquake (EQ) occurred in the years 2012 and 2011, respectively. A running median of the foF2 and linked inter quartile range (IQR), upper bound (UB) and lower bound (LB) are utilized as a reference for identifying abnormal signals during the earthquakes. The results show anomalous reductions and enhancements in the foF2 within 7 days before and after the earthquakes. A comparative study between ionosonde retrieved and IRIPLAS-2011 model derived foF2 values reveals that the ionosonde retrieved values exhibit better anomalies during both the events. The analysis during extreme quiet geophysical conditions is shown to be a useful indicator of a forthcoming earthquake.

Introduction

The earthquake and its preparation process is terra incognita. The ionospheric effects created by earthquakes have appealed geophysicists' responsiveness for many years, due to the crucial need for the timely prediction of large earthquakes that cause massive destruction. Hence the ionospheric perturbations before large earthquakes occur are probed extensively by several geophysicists with traditional and novel approaches for earthquake predicting to save the lives. Ionospheric parameters trace out many spheres of our life. The first impulse of seismo-ionospheric coupling was commenced by Good Friday Alaska tremor in 1964 on March 27. This elongated history of seismo-ionospheric coupling studies can be traced in these reviews (Liu et al., 2004, Pulinets and Boyarchuk, 2004, Tramutoli et al., 2005, Parrot, 2009, Oyama et al., 2011).

A rise in the critical frequency of the F-layer (foF2) two days before and   fall in the critical frequency one day after the main shock was witnessed by Fatkullin et al., (1989). Again Liu et al., (2001) and Chuo et al., (2002) have noted the foF2 disparities related to Taiwan earthquakes and isolated precursors (afternoon reductions) 1–6 days prior to the main shocks. A total of 736 M>6:0 earthquakes global during 2002–2010 were statically studied using TEC/foF2 data, and the feature of Local Time (LT) variant in ionospheric anomalies was established (Le et al., 2011).

Dutta et al., (2007) also using a ground based ionosonde system, diagnosed strong ionospheric agitations over Delhi a few days preceding to the deadly 26 December 2004 Sumatra quake.

Although foF2 measurements have been carried out at a number of stations some models were used like regional models (Bradley, 1999; Hanbaba,1999), URSI model (Fox and McNamara, 1988), VOACAP Model (Rush,1986), CCIR (Bradely, 1990), International Reference Ionosphere (IRI) (Bilitza, 2001, Bilitza and Reinisch, 2008), Reference Ionosphere extended towards the plasmasphere. (IRIPLAS) by Gulyaeva et al., 2012 were framed. The most momentous and usually used amongst these models is International Reference Ionosphere (IRI) Model. An ionospheric empirical model that can to be updated with different observational data sources is IRIPLAS-2011 Gulyaeva, 2010). IRIPLAS-2011 model, evaluates critical frequency values by analyzing its preset coefficient matrices till plasmasphere. Few of the model input parameters, such as sun spot number and geomagnetic coordinates are dysfunctional and kept constant in the data set. Some parameters in this model are choice range flags such as foF2, TEC. In this foF2 is investigated as input parameter. Output parameters of the model are layer TEC estimates and related critical values.

If we define parameter h as HmF2, n as critical frequency of the signal in layer, y as TEC data of that hour and p vector as non-optimized parameters such as selected receiver latitude, longitude, time, date, daily sun spot number and Kp index (Sun spot number and Kp index are database inputs

independent of user entries), model finds estimation vector as given

$\hat{y}=iriplas\ (h,n,p,y)$ (1)

**Determination of F2 Layer Parameters**

During day light, all ionosphere layers act but when ionization effect of Sun vanishes at nights, only F2 layer rests in spite of its declining electron density profile. So F2 layer is desirable to be sensibly examined. Chief two characterizing parameters of the F2 layer is HmF2 (km) and foF2 (MHz). Only electrical signals exceeding a critical frequency level can traverse the ionosphere and transmit into outer cosmos. Signals with minor frequencies gets refracted and reflected. Therefore, foF2 is very important in radio communication. IRIPLAS model, evaluates critical frequency and height values by investigating its preset coefficient matrices. If IRIPlAS is restructured with GPS-TEC, more realistic HmF2 and foF2 approximations can be accomplished. In Figure 1, the iterational optimization loop model for minimizing the TEC error is given.

Defining error vector **v** as the difference of observational data set **y** and IRI-PLAS TEC estimations for ŷ each hour of day,

$v=y-\hat{y}$ (2)

and minimizing error norm $\|v\|$ in an iterative loop hints us to optimized *h* and *f* parameters.

Proper adaption of Non-Linear Least Squares method for optimizing HmF2 and foF2 parameters and initializing the algorithm with HmF2 and foF2 estimations acquired from IRI-PLAS model (without using IONOLAB TEC) and running algorithm with IONOLAB TEC updates would lead to a meaningful explanation.
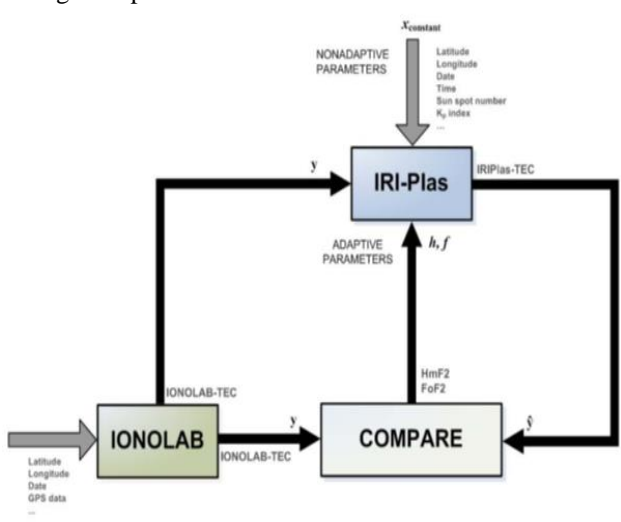

Figure 1. IRI-PLAS Iterative Optimization Model taken from IONOLAB (Cited: Şahin et al, 2011)

2. Data collection

For both the earthquakes, the geomagnetic indices AE,Dst,ap,kp are obtained from Kyoto, Japan. The hourly foF2 ionosonde data is recovered from Spidr NOAA and Ionolab.org gives hourly foF2 by IRIPLAS-2011 model.

For low latitude the ionosonde receiver station is Cocos Island (12.18°S, 96.98°E) which is 1665.2 km from the Sumatra epicenter whereas King Salmon (58.4°N,156.4°S) is the ionosonde receiver positioned at 1207km from the epicenter of mid-latitude Fox-Island earthquake. From IRIPLAS-2011 the respective data is retrieved from the same geographical coordinates as done for the same coordinates of real ionosonde data. Figure 2 presents the locations of the

earthquake epicenters (star) and foF2 data receiver stations (+), in geographic coordinates.
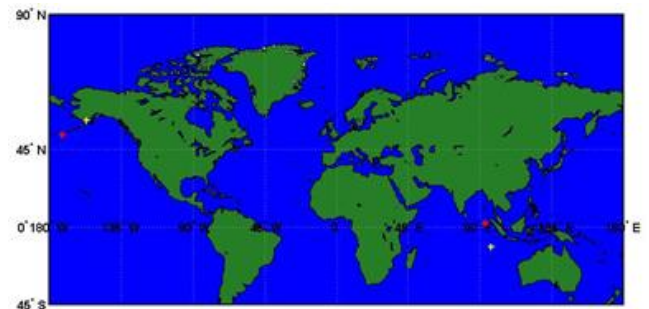
Figure 2. Geographic sites of the two earthquake epicenters (red star) and their respective Ionosonde receiver stations (yellow plus sign).

The magnitude, happening time, geographic coordinates of the epicenter, the radius of the earthquake preparation zone of these events and the geographical coordinate of the ionosonde receiver to collect foF2 hourly data and its distance from the earthquake are summarized in Table 1.

Magnitude (Richter scale)	Date of happening	Geographical coordinates of event		Geographical coordinates of Data collector station		Dobrovolsky range in km	Distance of receiver from the epicenter in km
		Lat (°)	Long(°)	Lat (°)	Long(°)		
8.6	April 11, 2012	2.31°N	93.06°E	12.18°S	96.98°E	4989	1665
7.2	June 24, 2011	52.00°N	171.85°W	58.4°N	156.4°W	1250	1207

Table 1 Earthquakes magnitude, time of occurrence, geographical coordinates of data receiver and the epicenter along with their distance

3. Methodology

The earthquake preparation area formation was presented by Dobrovolsky et al., (1979) using the elastic deformation scheming. In this research we used the Dobrovolsky formula, within which receiver is located. The size of the earthquake preparation area depends on the earthquake magnitude.

The Dobrovolsky formula is $R=10^{0.43M}$

where

R=quake region radius

M=quake magnitude in Richter scale.

foF2 data, reclaimed from ionososnde lies in Dobrovolsky zone was analysed a week prior and later to each earthquake. It is well known that the ionosphere has many cycle instabilities. To identify abnormal signals, we compute running median $\overline{X}$ of foF2 for every single hour and the linked Inter Quartile Range(IQR) to construct the upper bound($\overline{X}$+ IQR) and lower bound ($\overline{X}$+IQR).These bounds are calculated during the tremor duration to separate seismic inconsistencies from prevailing variations (Liu et al., 2004). With the hypothesis of a normal distribution having median $\overline{X}$ and

standard deviation σ taken for the foF2, according to (Liu et al., 2004), the upper and lower bounds of IQR are estimated using the succeeding formulas.

IQR Upper bound (UB) = $\overline{X}$+1.34 σ

IQR Lower bound (LB) = $\overline{X}$-1.34 σ

If the foF2 value at this time point was higher than the UB or reduced than LB, it was demarcated as an abnormal point. To enumerate the ionospheric disorders, the percentage of foF2 deviation (ΔfoF2 %) has been considered from, both the bounds. This can be achieved by using following equations (Dabas et al., 2007), which is entitled as %deviation positive and %deviation negative

$$\Delta foF2\% \text{ (positive)} = \frac{foF2_{EQ}-IQR_{UB}}{IQR_{UB}} \times 100$$

If $foF2_{EQ} \leq IQR_{UB}$ then $\Delta foF2\%$ (positive) = 0

$$\Delta foF2\% \text{ (negative)} = \frac{foF2_{EQ}-IQR_{LB}}{IQR_{LB}} \times 100$$

If $foF2_{EQ} \geq IQR_{LB}$ then $\Delta foF2\%$ (negative) = 0

.

Where $foF2_{EQ}$ is the value of foF2 during earthquake period. Ionospheric variation caused by geophysical activity can promote amplification, or weakening, of the demonstration of seismo-ionospheric properties (e.g., Zakharenkova et al., 2007). So it must that Kp, Dst, Ap ,AE tot be analysed. To eliminate the option of irregularity detection during elevated and adequate geomagnetic commotion, the ΔfoF2% values with |Dst|>15 nT, ap>16 and -3<Kp<3 are strained out from the enquiry. We are doing calculations in quiet period so the threshold value of Dst<-15nT, and ap<16 are taken in our analysis for both the earthquakes.

3.1 Analysis of the ionospheric variations of the April 11, 2012, Sumatra earthquake

At 08:38 (Universal Time) UT with deepness of 22.9 km an earthquake struck on April 11, 2012at the off west coast of Northern Sumatra (2.311°N, 93.063°E), Indonesia having magnitude 8.6 (shown in Table 1). Strike-slip fault is blamed for this tremor surrounded by the marine lithosphere of the Indo-Australia plate. The tremor was sited 200 km to the southwest of the foremost subduction zone that defines the plate boundary amid the India/Australia along with Sunda plates coastal Sumatra. So, the India/Australia plate tend to shift north-northeast with respect to the Sunda plate at the rate of roughly 52 mm/yr.

Figure 3 grants Dst, Kp, Ap, and the foF2 variations with the associated upper and lower bounds for the observation period between 3 April to 18 April in 2012. The erect arrow in the Figure designates the time of the tremor. The horizontal black lines in Figure 3a–b show the threshold values of the Dst(-15 nT) and ap (16), respectively.

In Figure 3c & 3d, foF2 signal derived from ionosonde and IRIPLAS-2011, respectively with the upper and lower bounds are plotted using the method discussed in Section. 2. The foF2 signal was successful to surpass the upper and lower bounds in Figure 3c, but failed to surpass the upper bound in Figure 3d. The recognitions were witnessed at the vicinity of the epicenter. However, as indicated by the Dst, AE,Kp and ap indices in Figure 3a–b, the geomagnetic conditions on 6 and 12 April were upset, whereas the geophysical condition on 5,15,16,17,18 April were characterized as quiet. Therefore, only fof2 anomalies observed on are 5, 15, 16, 17,18 April are considered as possible pre-earthquake ionospheric anomalies, hence they are emphasized by the P alphabet besides the ones perceived on disturbed days are marked by the D alphabet as

depicted in Figure 3c.In Figure 3d the anomalies detected on disturbed day falls on 4,7 and 13 April, so they are shown as D character as the geophysical activities were disturbed on 4,7 and 13 April as revealed in Figure 3a–b whereas on 5,8,10,11,13 to18 April, during the quiet geomagnetic condition the perturbations are marked as P alphabet.
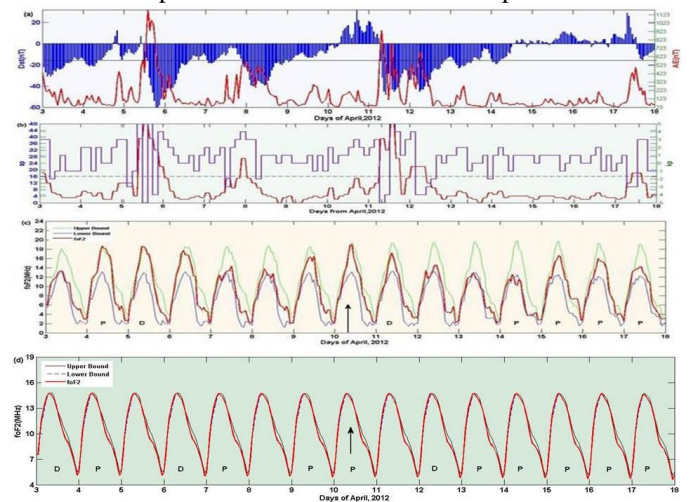
Figure 3. The geomagnetic indices (a) Dst and AE, (b) ap and Kp, and the, (c) foF2 variations and the associated upper and lower bounds between 3 April to 18 April 2012, at the epicenter (2.311°N, 93.063°E) obtained by ionosonde (d) foF2 variations and the associated upper and lower bounds between 3 April to 18 April 2012, at the epicenter (2.311°N, 93.063°E) obtained by IRIPLAS-2011 model.

Figure 4 shows the percentage of foF2 deviation for the same observation period presented in Figure 3. In Figure 4, the positive and negative values of the strained foF2% show the discrepancy pertaining to the upper and lower bound, respectively.
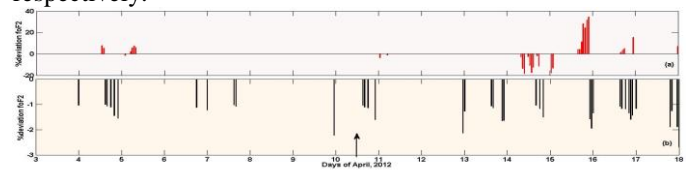

Figure 4. At the epicenter (2.311°N, 93.063°E) the percentage of foF2 deviation between 3 April to 18 April 2012. The positive and negative values show the filtered Δfof2% variations with respect to their upper and lower bound. (a) derived from ionosonde (b) Calculated from IRIPLAS-2011.

Referring to the days highlighted in Figure 4a, significant increases in ΔfoF2% of 1% to 34% were observed on 5, 15,16,17,18 April with respect to Figure 3c. Extreme crest amplification (34%) appears on 16 April, 2012 post to the 5th day of the EQ occurrence day at 22UT/4LT(Local Time) (LT=UT+6hr). Again with respect to Figure 3d significant increases in ΔfoF2% of about 1-2.7 % were observed with respect to Figure 4 on quiet days. Maximum trough amplification (2.7%) is witnessed on 18April after seven days of the shock at 24UTor 6LT.

3.2 Correlation analysis between foF2 values derived from Ionosonde and IRIPLAS-2011 model for Sumatra earthquake, 2012

Karl Pearson's coefficient of correlation calculated for foF2 real data and which is obtained from model is plotted in Figure 5. Calculation shows a high positive correlation coefficient which is equal to .9
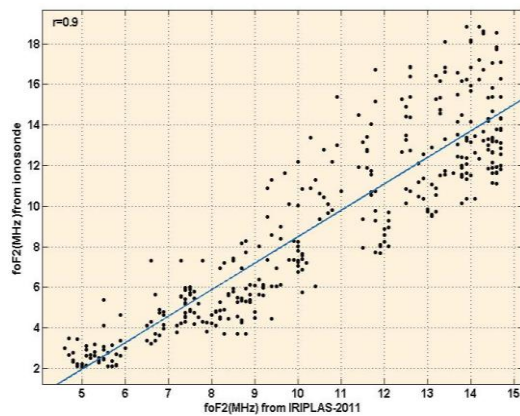
Figure 5. Correlation between foF2 values derived from IRIPLAS-2011 and ionosonde

4.1 Analysis of the ionospheric variations of the 24June, 2011 Fox Island earthquake

The Fox Island shake in Alaskaa hit in June 24. of magnitude 7.2 in 2011 at 03:09 UT arose at (52.00°N, 171.859°W), (shown in Table 1) due to seismic fault in the Pacific slab. This Pacific wedge dives base of the North America plate at the Aleutian Trench at the subduction zone thinning out to the southwest as of Alaska. This EQ is having its depth 63 km and mechanism acclaim that the earthquake befallen surrounded by the subducting plate, of the amalgamated zone flanked by North America in addition the Pacific. At the site of this happening, the Pacific plate meets with North America at a velocity of around 71 mm/yr towards northwest.

The indices Dst, Kp, Ap, and the foF2 variations with the associated upper and lower bounds for the observation period between 16June to 1 July 2011 are depicted in Figure 6. The upright arrow in the Figure symbols the EQ day. The flat black lines in Figure 6a–b display the verge values of the Dst and ap indices, which are -15 nT and 16, respectively.

In Figure 6c & 6d, foF2 signal derived from ionosonde and IRIPLAS-2011,respectively with the upper and lower bounds are plotted using the technique conversed in Section. 2. The foF2 signal was not successful to exceed the lower bound in Figure 6c, but it overdoes the upper bound. The estimations shows that this nonlinear signal was successful to outstrip the upper and lower bounds as depicted in Figure 6d. These detections were seen between the period of a week pre and post tremor activity at the neighborhood of the epicenter. However, as signposted by the Dst, AE, Kp and ap indices in Figure 6a–b, the geomagnetic activities during the days of 17, 19, 20, 21, 24, 26 to 30 June were considered as quiet, therefore, only foF2 variances observed on these quiet days are well-thought-out as possible pre-earthquake ionospheric anomalies, hence they are highlighted by the P character and no anomaly is found on disturbed days as shown in Figure 6c. Now In Figure 6d the foF2 inconsistencies detected on disturbed day falls only on 1July, so it is presented as D character as the geophysical activities were disturbed on this day as shown in in Figure 6a–b whereas on 19,25,29,30 June & 1 July, 2011, during the quiet geomagnetic conditions, which are revealed in Figure 6a–b, the perturbations are marked as P alphabet.
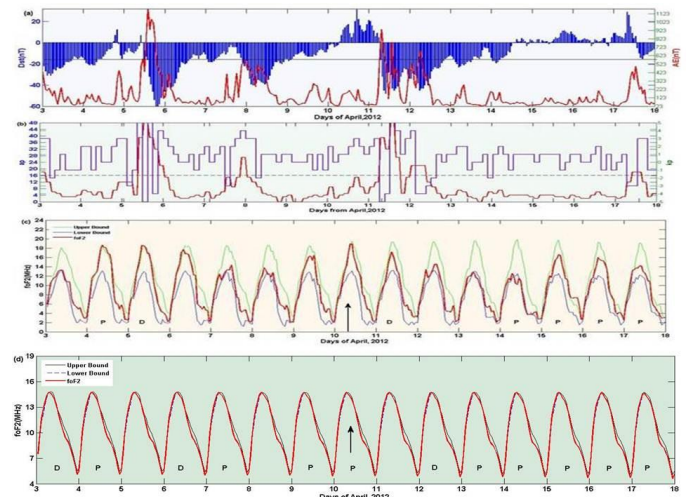
Figure 6. The geomagnetic indices (a) Dst and AE, (b) ap and Kp, and the (c) foF2 discrepancies and the related upper and lower bounds between 16 June to 1 July 2011, at the epicenter (52.00°N, 171.859°W), obtained by ionosonde (d) foF2 disparities and the linked upper and lower bounds between 16 June to 1 July 2011, at the epicenter (2.311°N, 93.063°E), detected by IRIPLAS-2011 model.

Figure 7 displays the percentage of foF2 deviation for the same observation period presented in Figure 6. In this Figure, the positive and negative values of the filtered foF2% show the discrepancy with respect to the upper and lower bound, respectively.

Referring to the days highlighted in Figure 7a, significant increase in ΔfoF2% of nearly 1−16% was observed on 17, 19, 20, 21, 24, 26 to 30 June with respect to Figure 6c. Extreme crest intensification (16%) appears on 28 June, 2011 after the 4th day of the EQ occurrence day at 19UT/10LT (LT=UT-9hr). Again with respect to Figure 6d significant increases in ΔfoF2% of about 1-1.2 % were witnessed with respect to Figure 7b on 19,25,29,30 June & 1 July, 2011. Maximum crest amplification (1.13%) is witnessed on 25June, after 1 day of the shock at 3UTor at 6LT on 24 June, same day of the shock.
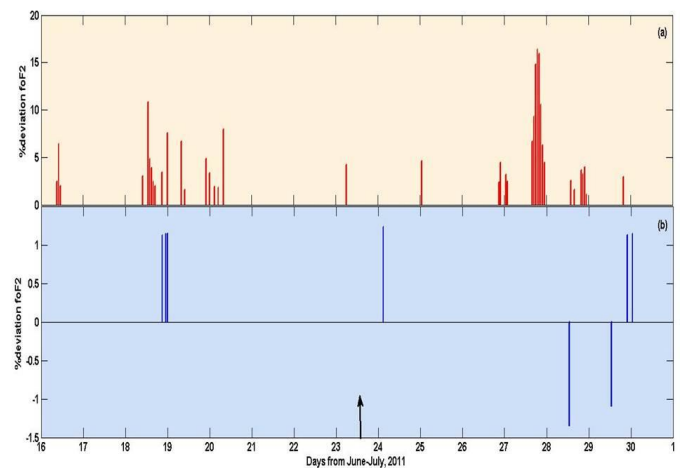
Figure 7. At the epicenter (52.00°N, 171.859°W), the percentage of foF2 deviation between 16 June to 1July, 2011. The positive and negative values illustrate the filtered ΔfoF2% variations with respect to their upper bound and lower bound. (a) derived from ionosonde (b) Calculated from IRIPLAS-2011.

4.2 Correlation analysis between foF2 values derived from Ionosonde and IRIPLAS-2011 model for Fox Island earthquake

Karl Pearson's coefficient of correlation is calculated for foF2 real data and which is obtained from model is plotted in Figure 8. Calculation shows a moderate correlation coefficient which is equal to .48
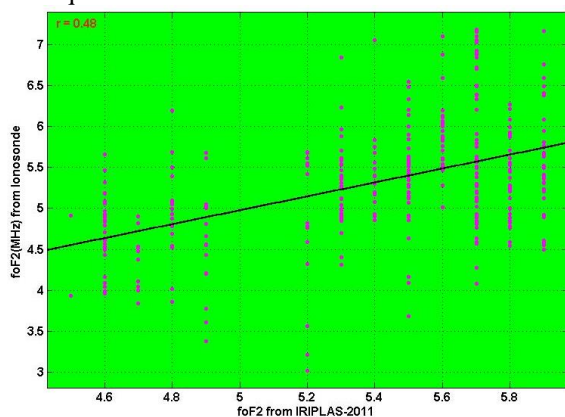
Figure 8. Correlation between foF2 values derived from IRIPLAS-2011 and ionosonde

5. Conclusions

Based on the present investigations, the main features of the study are listed below:

(1)By investigating the critical frequency of F2 layer retrieved from Ionosonde & IRIPLAS-2011 model for the two earthquakes of low & mid latitude of M8.6 &7.2 extreme quiet period we notice that the anomalous variations in foF2 are soundly correlated with the shock, in the Dobrovolsky zone.

(2) Our results show that positive and negative anomalies were observed by analyzing real data of the low latitude Sumatra earthquake. Extreme peak enlargement (34%) seems on 16 April, 2012 after the 5th day of the EQ occurrence day at 4LT. Again with respect to IRIPLAS-2011 model, for this low latitude earthquake we found only negative glitches persists with supreme crib amplification (2.7%) on 18April afterwards 7 days of the shock at 6LT. This means that extreme enhancements are witnessed in early morning hours after the earthquake occurrence day from real ionosonde data & model data. There is a difference of maximum value of percentage enhancement from both data sources. The reason can be interpreted as IRIPLAS-2011 model data is estimated from GPS TEC, which gives TEC values of topside, bottom side and plasmasphere, further which is sensitive to topside and plasmasphere while ionosonde gives TEC/foF2 values of lower layer and upper layer of the ionosphere up to 1000km. this finding is consistent with the research report of Belehaki., et al., in 2003 who studied the TEC data from GPS and ionosonde and found values differ especially during night which can be blamed to the plasmaspheric storm.

(3) The Fox Island earthquake analysis from ionosonde retrieved values tells only prominent positive perturbations were portrayed, with maximum positive perturbation of 16% was evident after 4 days of occurrence of earthquake at 10 LT. Again the analysis of this event from model data reveals the existence of both positive and negative anomalies with maximum peak amplification (1.13%) at the day of the shock at 6 LT. Thus maximum peak is during morning hours from both real and model data. (4) Correlation between real and model data for the parameter foF2 revealed a high correlation between both the data retrieval sources for Sumatra Island earthquake. Hence the model prove to be reliable for analysis, but in case of Fox Island earthquake positive and moderate

correlation is obtained. From analysis of Fox Island quake, we infer that Ionosonde real data shows maximum anomalous percentage deviation of foF2 data and prove to be more reliable. Hence IRIPLAS Model needs to be improved.

A discrepancy between IRIPLAS-2011 derived data with the real observations at low and mid latitude regions is found. These results might be useful for the model improvement and the model error representation of the data assimilation.

References

● Belehaki, A., N. Jakowski, and B. W. Reinisch, Comparison of ionospheric ionization measurements over Athens using ground ionosonde and GPS-derived TEC values, Radio Sci., 38(6), 1105, doi:10.1029/2003RS002868, 2003.

● Bilitza D., International Reference Ionosphere, Report NSSDC 90-22. National Space Science Data Centre/ World Data Centre A for Rockets and Satellites, Greenbelt, MD, USA, 1990.

● Bilitza, D. (2001). International reference ionosphere 2000, Radio Sci., 36 (2), 261-275.

● Bilitza, D., and B.W. Reinisch (2008). International reference ionosphere 2007 improvements and new parameters, Adv. Space Res., 42 (4), 599-609.

● Rush, C. M. (1986).Ionospheric Radio Propagation Models and Predictions-A Mini-Review, IEEE Trans. Antennas Propag. AP-34, 1163 .

● Chuo, Y.J., Liu, J.Y., Pulinets, S.A. and Chen, Y.I., 2002, The ionospheric perturbations prior to the Chi-Chi and Chia-Yi earthquakes. Journal of Geodynamics, 33, pp. 509– 517.

● Dobrovolsky, I. R., S. I. Zubkov, and V. I. Myachkin, Estimation of the size of earthquake preparation zones. Pure Appl. Geophys, 1979; 117: 1025–1044

● Dutta, H.N., Dabas, R.S., Das, R.M., Sharma, K. and Singh, B., 2007, Ionospheric perturbations over Delhi caused by the 26 December 2004 Sumatra Earthquake. International Journal of Remote Sensing, 28, pp. 3141–3151.

● Fatkullin, M.N., Zelenova, T.I. and Legenka, A.D., 1989, on the ionospheric effects of asthenospheric earthquakes. Physics of the Earth and Planetary Interiors, 57, pp. 82–85.

● Gonzalez WD, Joselyn JA, Kamide Y, Kroehl HW, Rostoker G, Tsurutani BT, Vasyliunas VM (1994) What is a geomagnetic storm? J. Geophys Res. 99: 5771-5792.

● Hanbaba, R. (1999), Improved quality of services in iono-spheric telecommunication systems planning and operation, Action 251, final report, Eur. Coop. in the Field of Sci. and Tech. Res. (COST), Space Res. Cent., Warsaw, Poland.

● Le, H., Liu, J. Y., and Liu, L. 2011: A statistical analysis of ionospheric anomalies before 736 M6.0C earthquakes during 2002–2010, J. Geophys. Res., 116, A02303, doi:1 0.1029/ 2010JA015781.

● Liu, J.Y., Chen, Y.I., Chuo, Y.J. and Tsai, H.F., 2001, Variations of ionospheric total electron content during the Chi-Chi earthquake. Geophysical Research Letters, 28, pp. 1383–1386.

● Liu, J.Y., Chuo, Y.J., Shan, S.J., Tsai, Y.B., Chen, Y.I., Pulinets, S.A. and Yu, S.B., 2004, Pre-earthquake ionospheric

anomalies registered by continuous GPS TEC. Annales Geophysicae, 22, pp. 1585–1593.

● M. W. Fox and L. F. McNamara, Improved World-Wide Maps of Monthly Median foF2, J. Atmos. Terr. Phys. 50, 1077, 1988.

● Osella, A., Favetto, A. and Silbergleit, V., 1997, A fractal temporal analysis of moderate and intense magnetic storms. Journal of Atmospheric and Solar–Terrestrial Physics, 59, pp. 445–451.

● Oyama, K.I., Kakinami, Y., Liu, J Y., Abdu, M.A and Cheng, C Z. Latitudinal distribution of anomalous ion density as a precursor of a large earthquake. J Geophys Res ,2011; 116: A04319, doi: 10.1029/2010JA015948.

● Bradely, P.A 1990.: Mapping the Critical Frequency of the F2-Layer: Part 1-Requirements and Developments to Around 1980, Adv. Space Res. 10, #8, 47, 1990.

● Parrot M. 2009: Anomalous seismic phenomena: View from space in electromagnetic phenomena associated with earthquakes. In: Hayakawa M ed. Electromagnetic Phenomena Associated with Earthquakes Transworld Research Network, Trivandrum, India, Chapter 8, 205–234.

● Pulinets, S. A. and Boyarchuk, 2004: K. A. Ionospheric precursors of Earthquake. Springer, Berlin Germany, 315p.

● O. Sahin, U. Sezen, F. Arıkan, O. Arikan,2011. "Optimization of F2 layer parameters using IRI-Plas model IONOLAB Total Electron Content", Proceedings of RAST-2011, 2011

● Gulyaeva, T.L. 2010. "Storm time behavior of topside scale height inferred from the ionosphere-plasmasphere model driven by the F2 layer peak and GPS-TEC observations," *Advances in Space Research,* doi:10.1016/j.asr.2010.10.025, 2010.

● Gulyaeva, T.L., F. Arıkan, M. Hernandez-Pajares, I. Stanislawska, U. Sezen, "Assimilating the IRI-Plas model to the ionospheric hourly maps of GPS-TEC to produce the artificial foF2 and hmF2 global maps", 39th COSPAR Scientific Assembly, 2012

● Tramutoli, V., Cuomo, V., Filizzola, C., Pergola, N and Pietrapertosa C. Assessing the potential of thermal infrared satellite surveys for monitoring seismically active areas. The case of Kocaeli [Izmit] earthquake, August 17th, 1999. Remote Sensing of Environment, 2005; 96: 409–426.

● Zakharenkova, I. E., Shagimuratov, I. I., Krankowski, A., and Lagovsky, A. F.2007: Precursory phenomenon observed in the total electron content measurements before great Hokkaido of September 25, 2003 (M = 8.3), Stud. Geophys. Geod., 51, 267–278.